Kasetsart J. (Nat. Sci.) 48 : 263 - 282 (2014)

Effect of Mechanical Axis on Strain Distribution after Total Knee Replacement

Panya Aroonjarattham[1,*], Kitti Aroonjarattham[2] and Chakrit Suvanjumrat[1]

ABSTRACT

A total knee replacement is one of the most successful orthopedic procedures to enable the patient's return to a normal, active lifestyle. The angle of the mechanical axis depends on the surgeon's decision, which effects the strain distribution on the femoral bone and may lead to a fracture of the femur . This study evaluated the equivalent total strain on the femoral shaft under daily activities using various models of the lower extremity with a varus knee deformity and the lower extremity with a total knee prosthesis, which was inserted at five different angles—0°, 3° valgus, 5° valgus, 3° varus and 5° varus. The results showed that the insertion of a total knee replacement in the case of a bowleg helped to reduce the equivalent total strain on the bone. The position of the prosthesis with a 3° valgus angle produced less strain distribution on the femoral bone. From the results, the mechanical axis affected the risk of the bone fracture. Considering the plastic spacer, it was found that there was an increase in the von Mises stress in the medial side of the model leg with a knee prosthesis of 3° valgus .

Keywords: total knee replacement, mechanical axis, finite element analysis

INTRODUCTION

Osteoarthritis is the most common type of arthritis and one of the most common causes of knee pain (Mandelbaum and Waddell, 2005). Knee osteoarthritis is a disease usually found in older or middle-aged persons, especially in women; excessive body weight is a risk factor for increasing the onset of knee osteoarthritis (Pollard *et al*., 2008). Total knee replacement also called total knee arthroplasty is a highly successful surgical procedure that can relieve the pain and restore the function of an arthritic knee (American Academy of Orthopaedic Surgeons, 2011). During knee replacement, a surgeon removes the damaged bone and cartilage from the femur, the tibia and the tibia plateau and then cuts the distal femoral bone surface to the shape of the knee prosthesis and attaches the total knee prosthesis with the best fit to the thigh bone, shin bone and knee cap as shown in Figure 1.

The total knee replacement will change the mechanical axis of the lower extremity to relieve the patient's pain. The incidence rate of hip fracture after total knee replacement may be related to mechanical axis deviation resulting in strain distribution on the femoral bone (Daniel *et al*., 2011).

This study evaluated the effects of valgus and varus angles of the mechanical axis using the finite element method for a bowlegged patient after knee joint surgery.

1 Department of Mechanical Engineering, Faculty of Engineering, Mahidol University, Nakhon Pathom 73170, Thailand.

2 Department of Orthopaedics, Faculty of Medicine, Burapha University, Chonburi 20131, Thailand.

* Corresponding author, e-mail: panya.aro@mahidol.ac.th

Received date : 02/07/13 Accepted date : 21/11/13

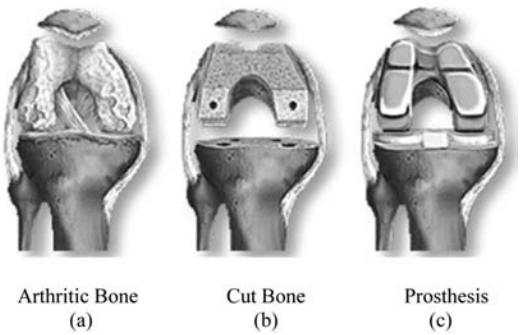

Figure 1 Total knee replacement: (a) Arthritis of knee joint (b) Removal of damaged bone; (c) Replacement with artificial knee. (University of Maryland Medical Center, 2011).

MATERIALS AND METHODS

Three-dimensional model of the femoral and tibia bones

The lower extremities, including the femur and tibia were scanned by a computerized tomographic (CT) scanner (GE LightSpeed VCT; Chonburi, Thailand). The three-dimensional solid model of the femur and tibia was created by the ITK-SNAP software (Version 2.4.0; Nov 21, 2012; grant R03 EB008200; USA) which consists of multiple image layers. A different threshold was used to evaluate the inner and outer contours of the bone model. To adjust the threshold, the light intensity was used to distinguish the cortical bone from the surrounding material as shown in Figure 2.

The completed three dimensional models of the bone were reconstructed as shown in Figure 3.

Total knee prosthesis model

Since a total knee prosthesis reflects an X-ray beam, a resin model of the total knee prosthesis was used for the CT scan as shown in Figure 4.

The three-dimensional models were refined as shown in Figure 5.

Ligament model

Three dimensional models of the ligament and meniscus were created using the SolidWork 2010 package (Version 2010; Mahidol University; Nakhon Pathom, Thailand)**.** The ligament model was composed of the anterior cruciate ligament, posterior cruciate ligament, lateral collateral ligament and medial collateral ligament. The

Figure 2 Sliced image of lower extremity with thresholding of femur and tibia.

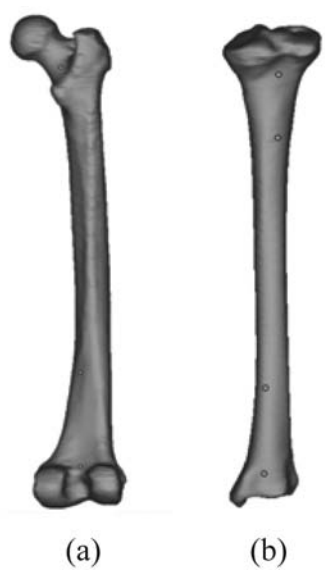

Figure 3 Three-dimensional model: (a) Femur; (b) Tibia.

three-dimensional models were used to reconstruct and locate the knee joint in the desired anatomical position as shown in Figure 6.

Virtual simulation

A virtual simulation technique was used to integrate the model of a knee prosthesis into the bone model with the actual surgery position of the total knee replacement to apply finite element analysis. The total knee prosthesis insertion was simulated with five different models by varying the amount of the varus and valgus angles of the knee. The conditions of neutral alignment (0°), 3°varus, 5°varus, 3°valgus and 5°valgus are shown in Figure 7.

This study focused on the strain distribution on the femur, especially the maximum strain on the femoral neck and shaft after knee arthroplasty that can effect a femoral bone fracture. The valgus and varus angle about the mechanical axis after knee joint surgery may be determined by the surgeon's experience, which may lead to a fracture of the femur. All cases studied are shown in Table 1.

Mesh generation and convergence testing

All models were generated as mesh models with four-node tetrahedral elements using MSC Marc (Version 2010; Mahidol University; Nakhon Pathom, Thailand). The implant model had a total of 56,780 nodes and 245,867 elements. The femur model had a total of 36,382 nodes and 144,442 elements. The tibia model had a total of 27,406 nodes and 111,088 elements. The ligament

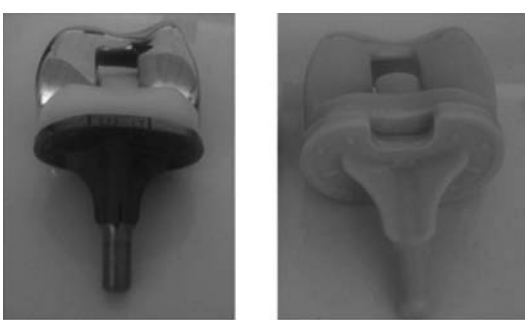

(a) (b)

Figure 4 Model of: (a) Total knee prosthesis; (b) Resin model of total knee prosthesis.

(a) (b) (c)

Figure 5 Three-dimensional models of knee prosthesis: (a) Femoral component, (b) Tibia component; (c) Plastic spacer.

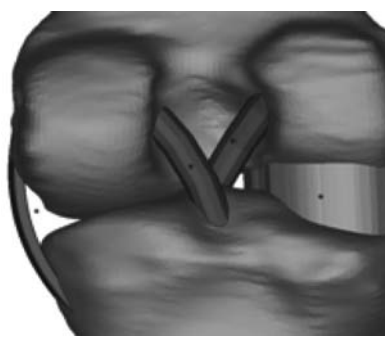

Figure 6 Three dimensional models of ligament and meniscus**.**

(a) (b) (c) (d) (e) (f)

Figure 7 Six models comparing the mechanical axis: (a) Model of 5° knee varus, (b) Model of 3° knee varus, (c) Model of 0° knee joint, (d) Model of 3° knee valgus, (e) Model of °knee valgus; (f) Model of bowleg with knee varus.

model had a total of 11,941 nodes and 47,140 elements. The bone-implant models are shown in Figure 8.

A reduction in the mesh size increases the computation time in finite element analysis. Convergence testing is a method to find the minimum mesh size that gives the exact solution and take the least calculation time. The mesh size was varied from 0.5 to 0.6, 0.7, 0.8, 0.9, 1.0 and 1.2 mm. The results of the equivalent total strain versus the mesh size are shown in Figure 9 and the optimal mesh size used in this study was 0.8 mm.

Material properties

The material properties of the cortical bone, cancellous bone, ligament and total knee prosthesis were assumed to be homogeneous, isotropic and linear elastic as shown in the Table 2.

Boundary condition

The body weight is transmitted from the proximal to the distal part of the femur. The muscular force acting on the proximal part of femoral bone is dependent on the activities undertaken such as walking or climbing stairs (Heller *et al*., 2004). The position and magnitude

Table 1 List of conditions for mechanical axis angle in the analysis.

Case	Alignment	Mechanical axis angle	Total knee arthoplasty	Finite element loading
1	varus	Knee varus from CT	no	Walking
2	normal	0	yes	Walking
3	varus	3°	yes	Walking
4	varus	5°	yes	Walking
5	valgus	3°	yes	Walking
6	valgus	5°	yes	Walking
7	varus	Knee varus from CT	no	Climbing stairs
8	normal	0	yes	Climbing stairs
9	varus	3°	yes	Climbing stairs
10	varus	5°	yes	Climbing stairs
11	valgus	3°	yes	Climbing stairs
12	valgus	5°	yes	Climbing stairs

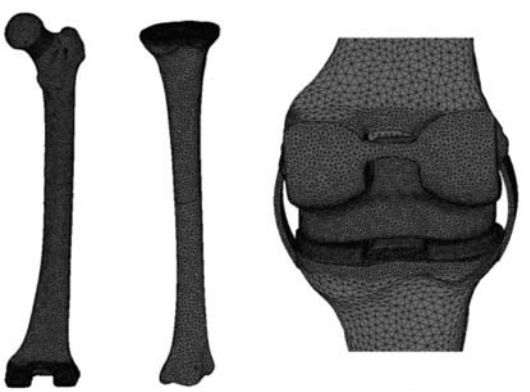

(a) (b) (c)

Figure 8 Mesh models of: (a) Femoral bone, (b) Tibia bone; (c) Total knee prosthesis.

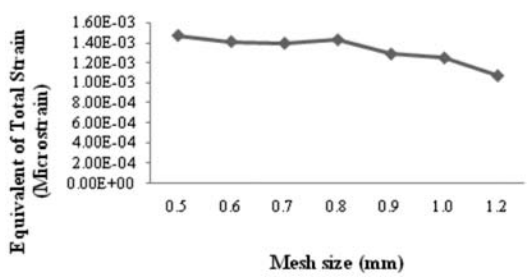

Figure 9 Mesh size and equivalent total strain in convergence testing.

of the forces acting on the bone are shown in Figure 10 and Table 3, respectively. The knee joint was placed with four ligaments to support the joint and to fix the model at the end of the tibial bone.

The MSC. program defined the relationship of the part contact under three conditions: no contact, touch contact and glue contact. The glue contact condition was applied to this research, where the underside total knee prosthesis contacts the bone cuts and the ligament contacts the bone. The glue contact was assumed to simulate an implant rigidly fixed as a result of bone ingrowths. The touch contact condition was applied to this research, where the plastic spacer contacts the femoral component and tibia component.

RESULTS

Finite element analysis was performed using the MSC software package to determine the total strain distribution on the femoral and tibia bones using six different models under daily activities such as walking and climbing stairs.

Table 2 Material properties of bone, ligament and prostheses (Bendjaballah *et al*., 1997; Weiss and Gardine 2001; Perez *et al*., 2008).

Material	Elastic modulus (MPa)	Poisson's Ratio
Cortical bone	14,000	0.30
Cancellous bone	600	0.20
menicus	12	0.45
ACL,PCL,LCL	345	0.40
MCL	332.2	0.40
Titanium	110,000	0.30
Cobalt-Chrome alloy	230,000	0.30
Polyethylene	1,000	0.45

ACL = Anterior cruciate ligament; PCL = Posterior cruciate ligament; MCL = Medial collateral ligament and LCL = Lateral collateral ligament.

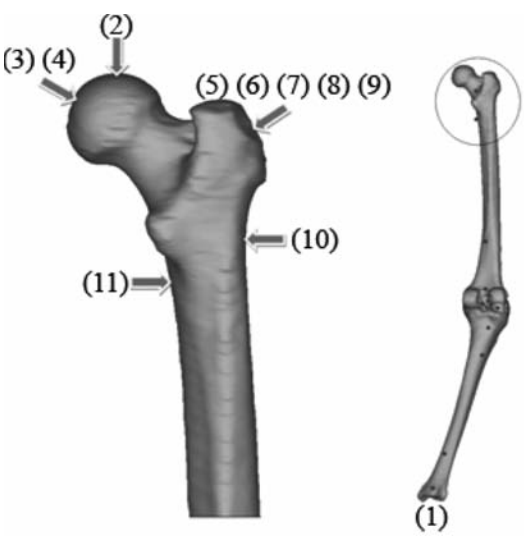

Walking
1. Fix
2. Body weight
3. Hip contact
4. Intersegmental resultant
5. Abductor
8. Tensor fascia latae, proximal part
9. Tensor fascia latae, distal part
10. Vastus laterallis

Climbing stairs
1. Fix
2. Body weight
3. Hip contact
4. Intersegmental resultant
5. Abductor
6. Ilio-tibial tract, proximal part
7. Ilio-tibial tract, distal part
8. Tensor fascia latae, proximal part
9. Tensor fascia latae, distal part
10. Vastus lateralis
11. Vastus mediallis

Figure 10 Muscular loading on the bone.

Table 3 Magnitude of muscular force on the proximal femur while walking and climbing stairs (Heller *et al.*, 2004).

Muscular force	Walking			Climbing stairs		
	x	y	z	x	y	z
1. Fix	0	0	0	0	0	0
2. Body weight	0	0	-836.0	0	0	-847.0
3. Hip contact	-54.0	-32.8	-229.2	-59.3	-60.6	-236.3
4. Intersegmental resultant	-8.1	-12.8	-78.2	-13.0	-28.0	-70.1
5. Aboductor	58.0	4.3	86.5	70.1	28.8	84.9
6. Ilio-tibial tract, proximal part	-	-	-	10.5	3.0	12.8
7. Ilio-tibial tract, distal part	-	-	-	-0.5	-0.8	-16.8
8. Tensor fascia, proximal part	7.2	11.6	13.2	3.1	4.9	2.9
9. Tensor fascia, distal part	-0.5	-0.7	-19.0	-0.2	-0.3	-6.5
10. Vastus lateralis	-0.9	18.5	-92.9	-2.2	22.4	-135.1
11. Vastus medialis	-	-	-	-8.8	39.6	-267.1

Strain distribution on femoral bone at medial side

Figures 11 and 12 show the equivalent total strain distribution on the femoral shaft on the medial side under conditions of walking and climbing stairs, respectively. Six different models were tested for a human leg with a total knee prosthesis with neutral alignment (0°), 3° varus, 5° varus, 3° valgus, 5° valgus and a human leg with a varus knee condition. The varus knee condition placed the highest total strain distribution on the medial side of the femoral bone, but when corrected with a total knee prosthesis, the total strain was decreased in all models.

Strain distribution on femoral bone on the lateral side

Figures 13 and 14 show the equivalent total strain distribution on the femoral shaft on the lateral side under conditions of walking and climbing stairs, respectively. Six different models were tested for a human leg with a total knee prosthesis with neutral alignment (0°), 3° varus, 5° varus, 3° valgus, 5° valgus and a human leg with a varus knee condition. The varus knee condition produced the highest total strain distribution on the lateral side of the femoral bone, but when corrected with a total knee prosthesis, the total strain was decreased in all models as occurred for the medial side. However, the lateral side received the tension load, so the total strain was higher than on the medial side.

Strain distribution on tibia bone on the anterior side

Figures 15 and 16 show the equivalent total strain distribution on the tibia shaft on the anterior side under conditions of walking and climbing stairs, respectively. Six different models were tested for a human leg with a total knee prosthesis with neutral alignment (0°), 3° varus, 5° varus, 3° valgus, 5° valgus and a human leg with a varus knee condition. The total strain distribution was similar in all models, with the most being in the shaft region of the tibia.

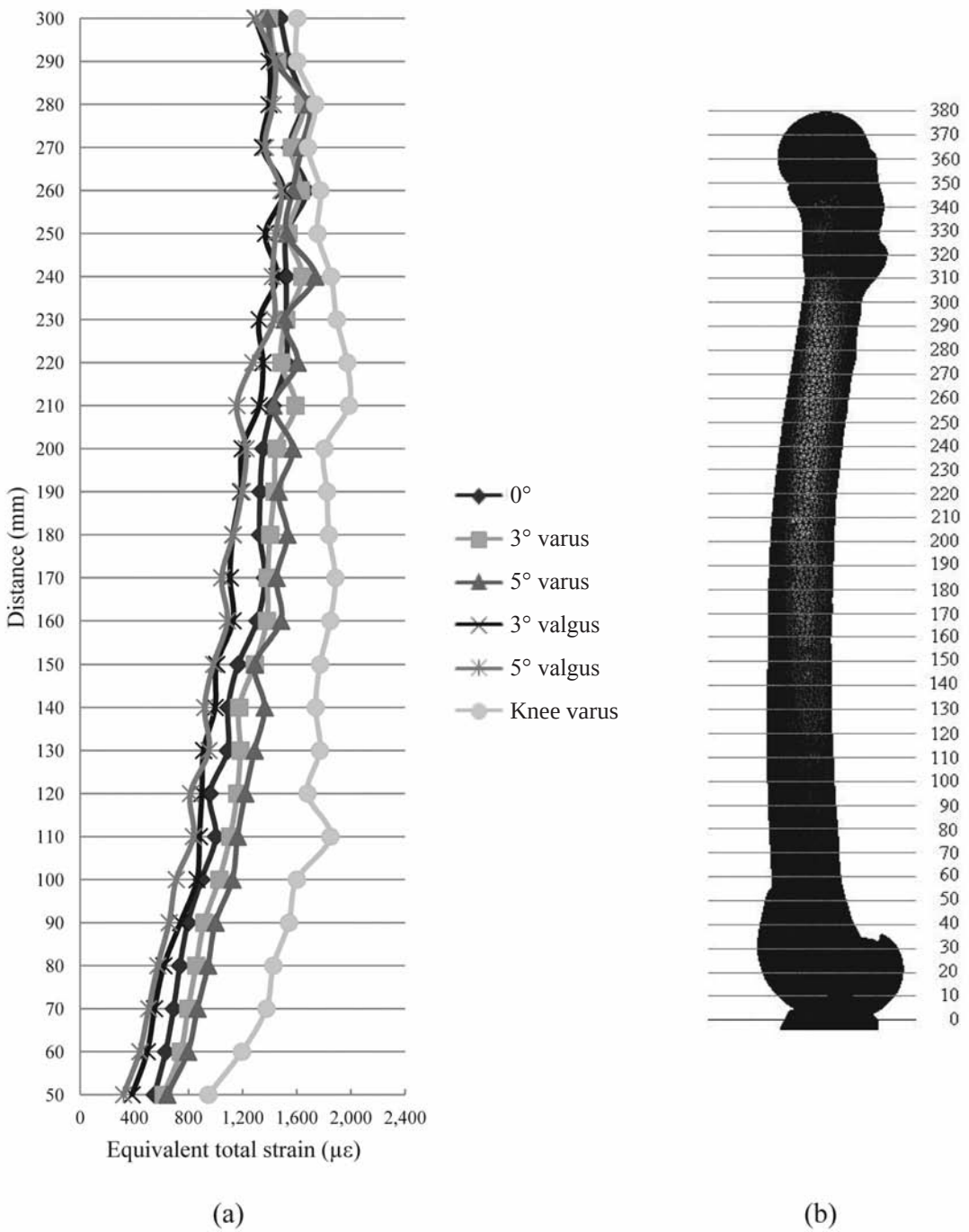

Figure 11 (a) Equivalent total strain on the femoral shaft on the medial side while walking; (b) Level on femoral bone from distal to proximal part.

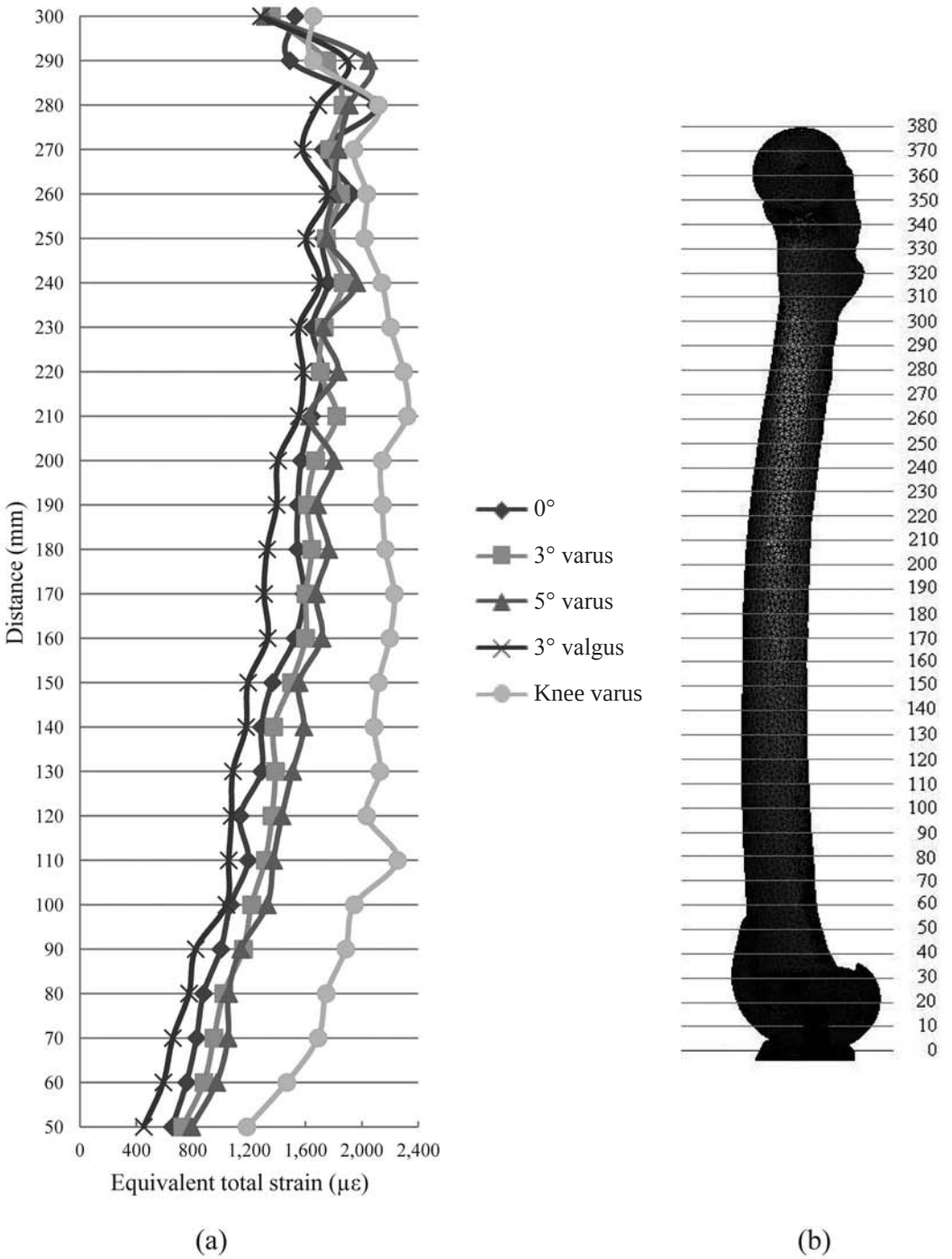

Figure 12 (a) Equivalent total strain on the femoral shaft on medial side while climbing stairs; (b) Level on femoral bone from distal to proximal part.

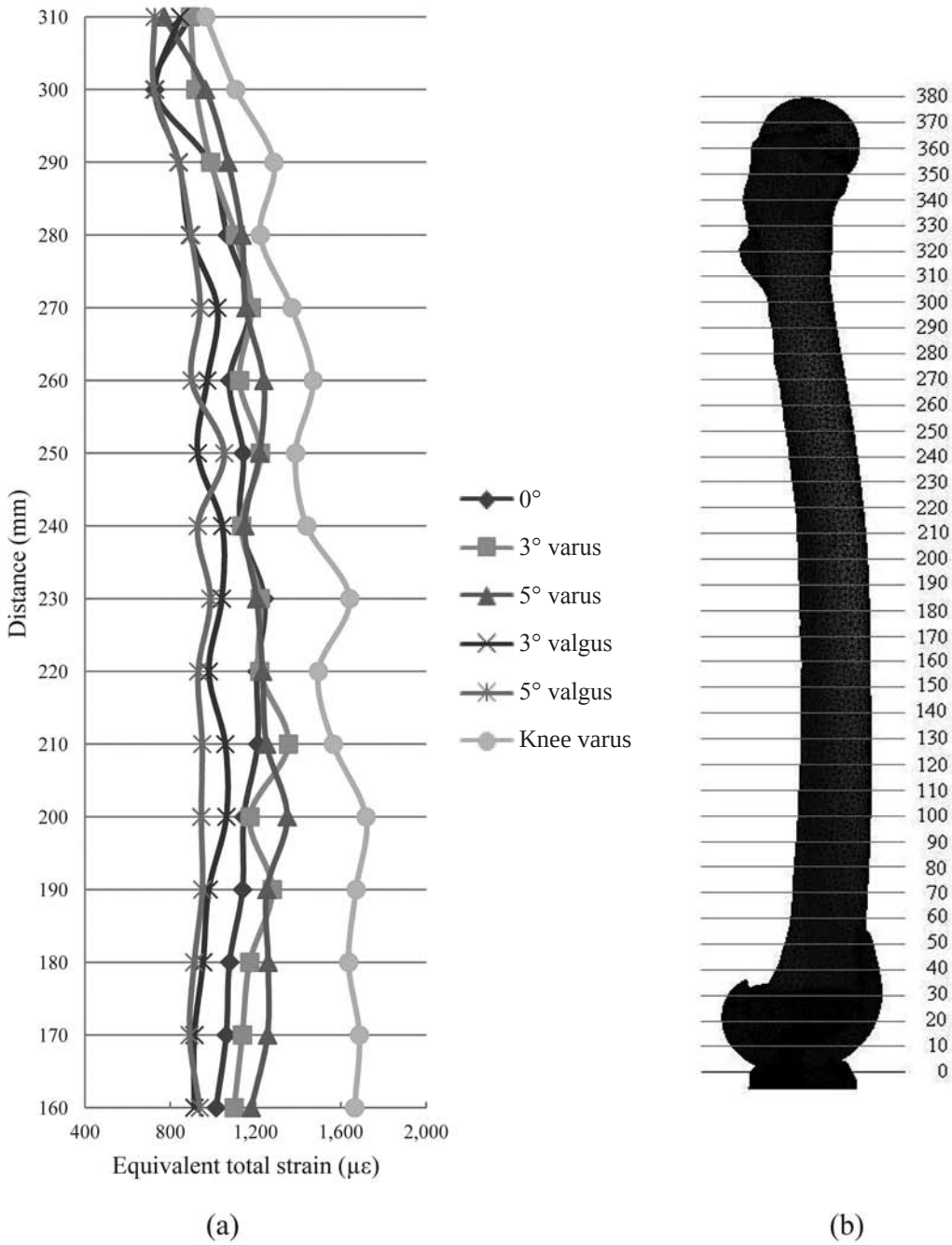

Figure 13 (a) Equivalent total strain on the femoral shaft on the lateral side while walking; (b) Level on femoral bone from distal to proximal part.

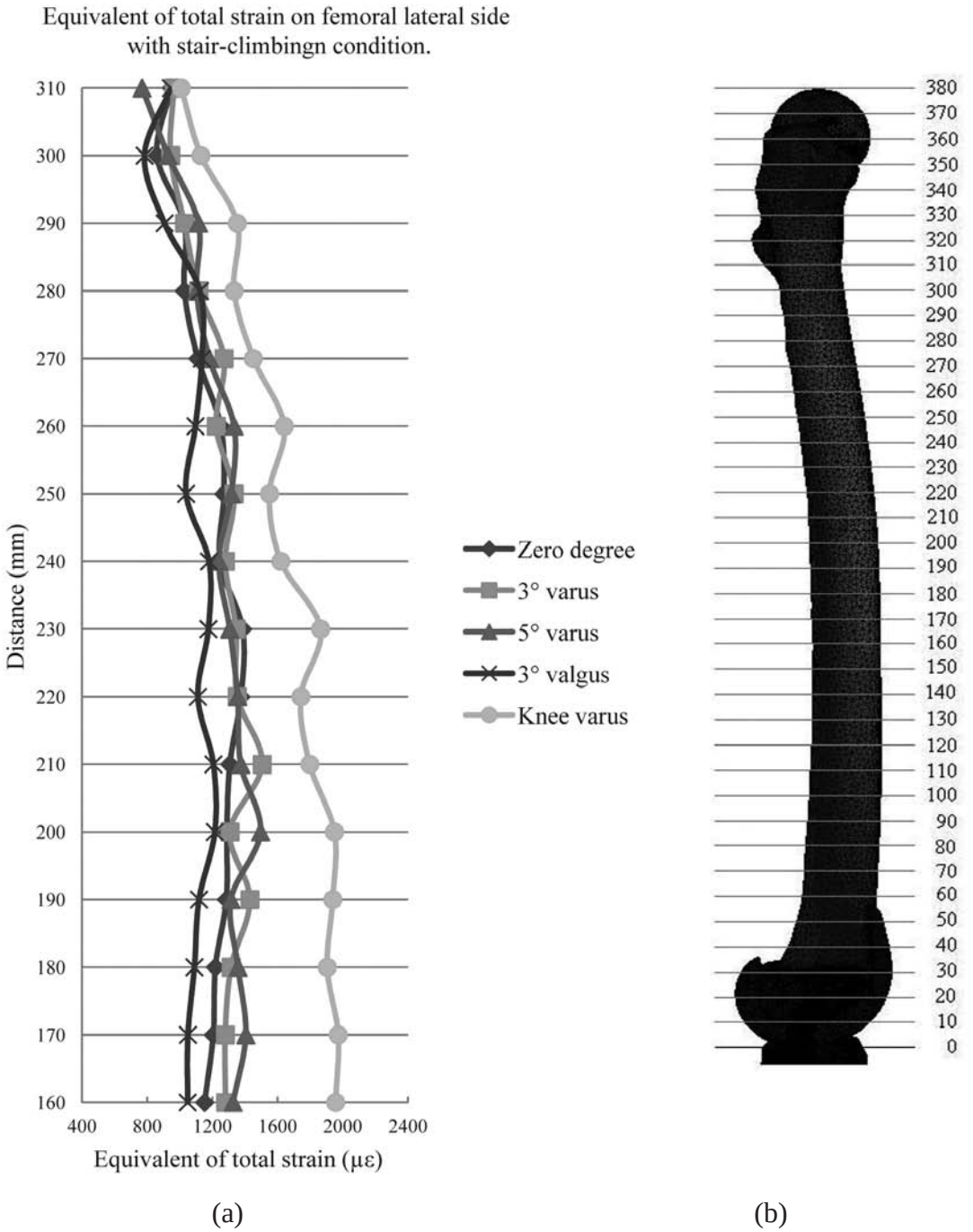

Figure 14 (a) Equivalent total strain on the femoral shaft on lateral side while climbing stairs; (b) Level on femoral bone from distal to proximal part.

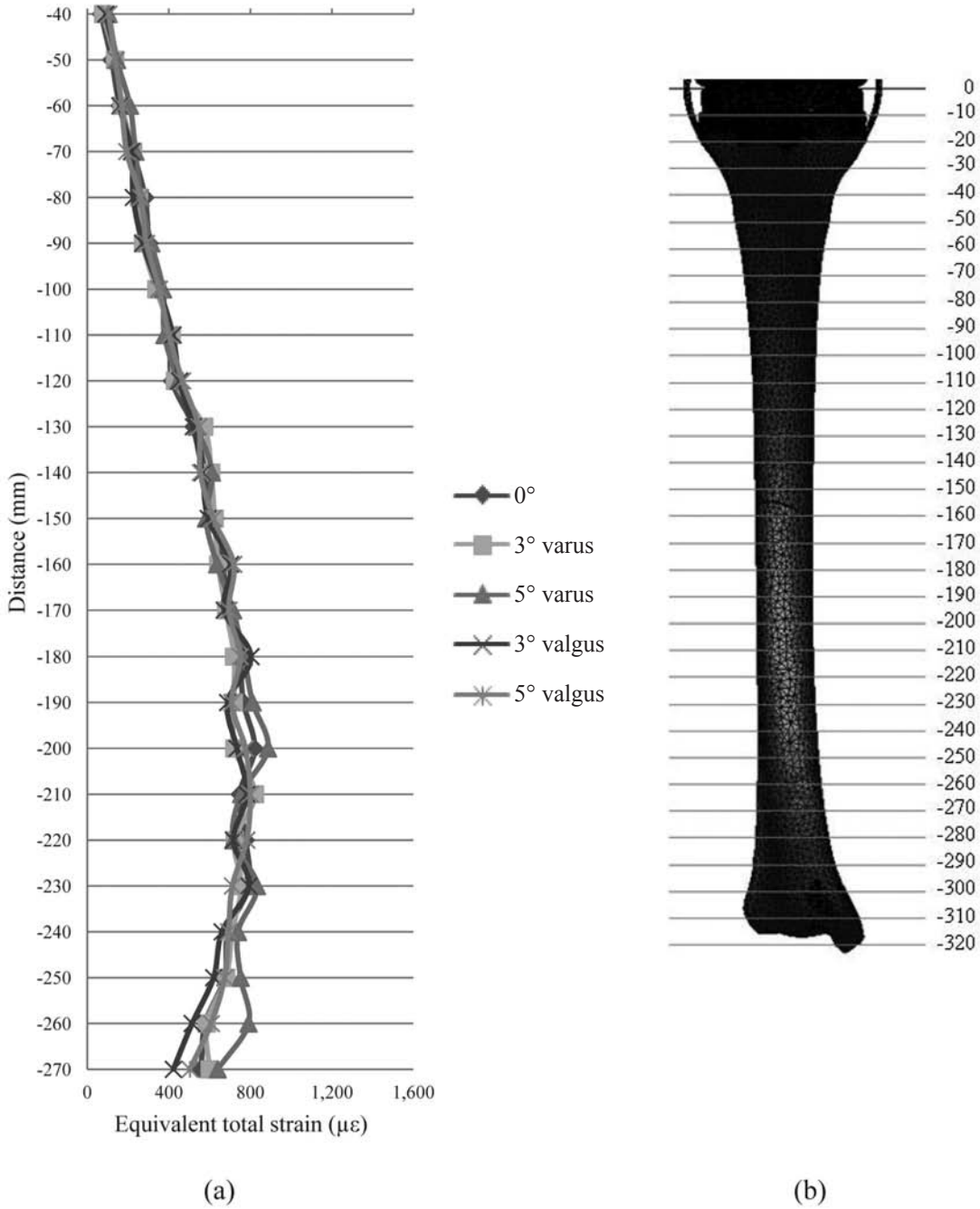

Figure 15 (a) Equivalent total strain on the tibia shaft on anterior side while walking; (b) Level on tibial bone from proximal to distal part.

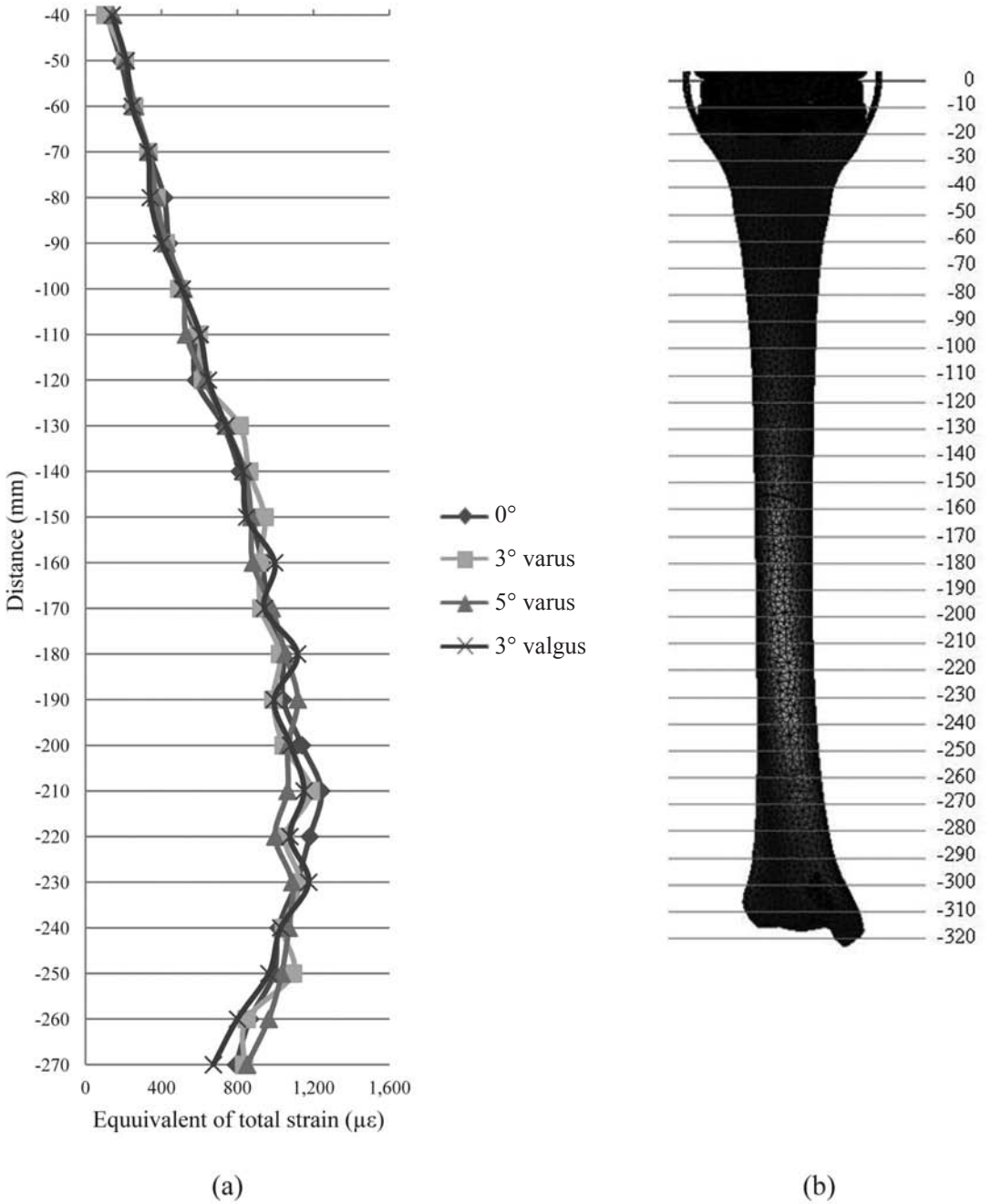

Figure 16 (a) Equivalent total strain on the tibia shaft on anterior side while climbing stairs; (b) Level on tibial bone from proximal to distal part.

Strain distribution on tibia bone on the posterior side

Figures 17 and 18 show the equivalent total strain distribution on the tibia shaft on the posterior side under conditions of walking and climbing stairs, respectively. Six different models were tested for a human leg with a total knee prosthesis with neutral alignment (0°), 3° varus, 5° varus, 3° valgus, 5° valgus and a human leg with a varus knee condition. The total strain distribution was similar in all models, with the most being in the distal region of the tibia.

DISCUSSION

The stress and strain distribution analysis using the finite element method is widely accepted as a useful technique to evaluate or predict the biomechanical behavior of orthopedic implants under certain load conditions (Helgason *et al.*, 2009; Amornsamankul *et al.*, 2010; Basafa *et al.*, 2013; Nishiyama *et al.*, 2013).

Femoral bone

The equivalent total strain on the femoral shaft, using the 6 models with daily activity are shown in Figures 19 and 20.

The average equivalent total strain distribution on the medial side of the femur with daily activity is shown in Table 4. The average strain distribution on the medial side under walking conditions with the varus knee, when compared with the model femur and 5° varus was decreased by 21%, with 3° varus was decreased 24%, with 0° was decreased 28%, with 3° valgus was decreased 37% and with 5° valgus was decreased 38%, while when climbing stairs, the same comparisons between the model femur with varus knee showed a decrease of 22% with the 5° varus, 26% with the 3° varus, 30% with 0° and a decrease of 36% with 3° valgus.

The average equivalent total strain distribution on the lateral side of the femur under daily activity is shown in Table 5. The average strain distribution on the lateral side under walking conditions with the model femur with a varus knee and 5° varus was decreased 27%, with a 3° varus was decreased 30%, with a 0° was decreased 34%, with a 3° valgus was decreased 43% and with a 5° valgus was decreased 46%. Under stair-climbing, the same comparison with the varus knee decreased 31% compared to the 5° varus, 32% compared to the 3° varus, decreased 36% with 0° and with the 3° valgus, it decreased 43%.

The model of the femur with a varus knee, showed decreased equivalent total strain distribution following insertion of a total knee prosthesis. The knee replacement did not affect the risk of a femoral bone fracture. The prosthesis with a 3° knee valgus angle produced less strain distribution on the femur than the other models but the appropriate position was the 0°prosthesis, which represented the anatomical position. The von Mises stress increased on the medial side of the plastic spacer in the 3° valgus model as shown in Figures 21 and 22 while walking and climbing stairs, respectively.

Positioning the implant depends on the surgeon's skills and experience. The results showed that a surgeon's conventional use of a 3° valgus angle in an operation causes high von Mises stress on the plastic spacer which results in its corrosion on the medial side, forcing femoral components and the mechanical axis back to the 0° prosthesis, which was the most natural angle for the human lower extremities. Apart from causing high von Mises stress on the plastic spacer, this conventional procedure also encourages an unnatural prosthesis degree; thus, it should be replaced by the use of a 0° prothesis.

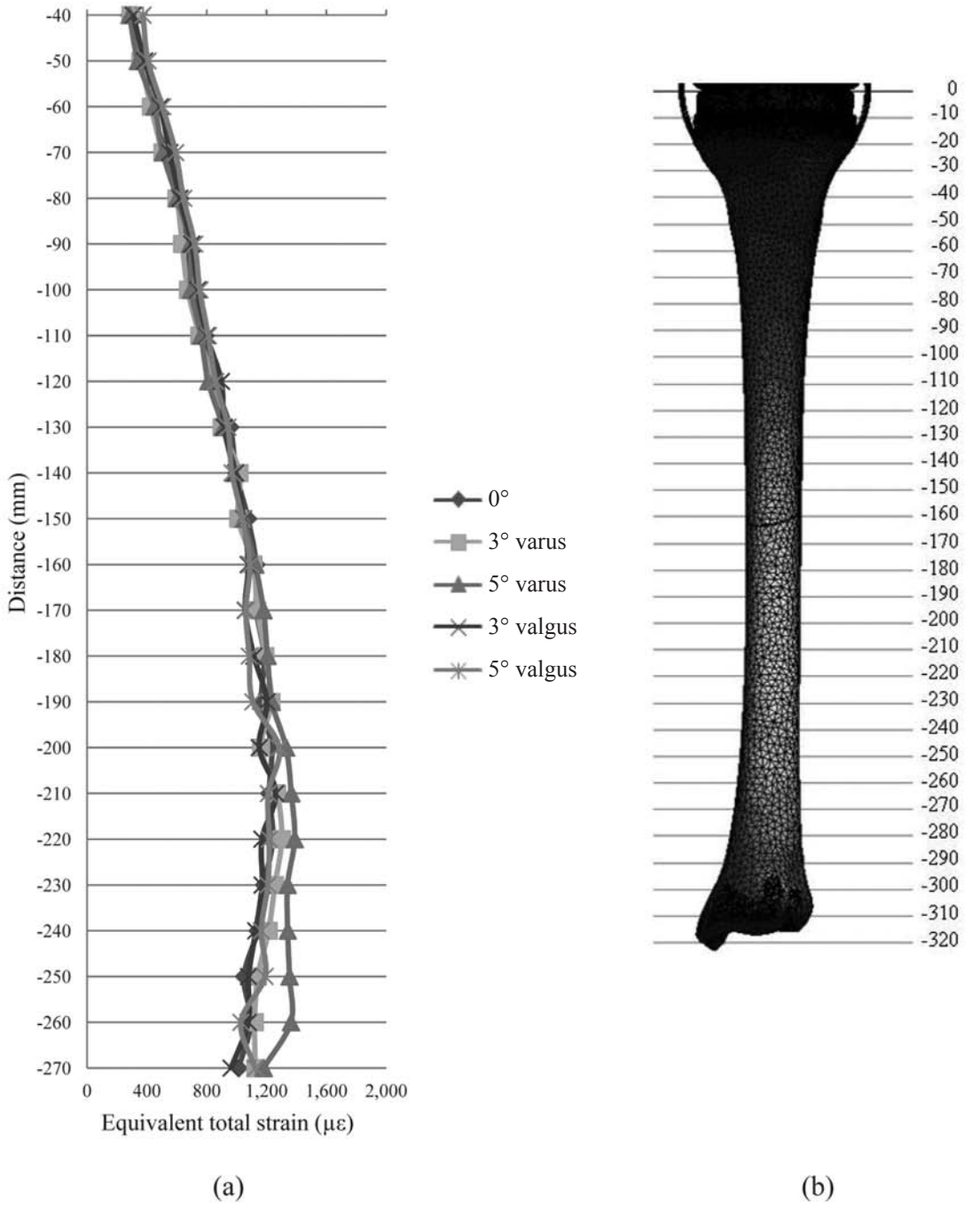

Figure 17 (a) Equivalent total strain on the tibia shaft on posterior side while walking; (b) Level on tibial bone from proximal to distal part.

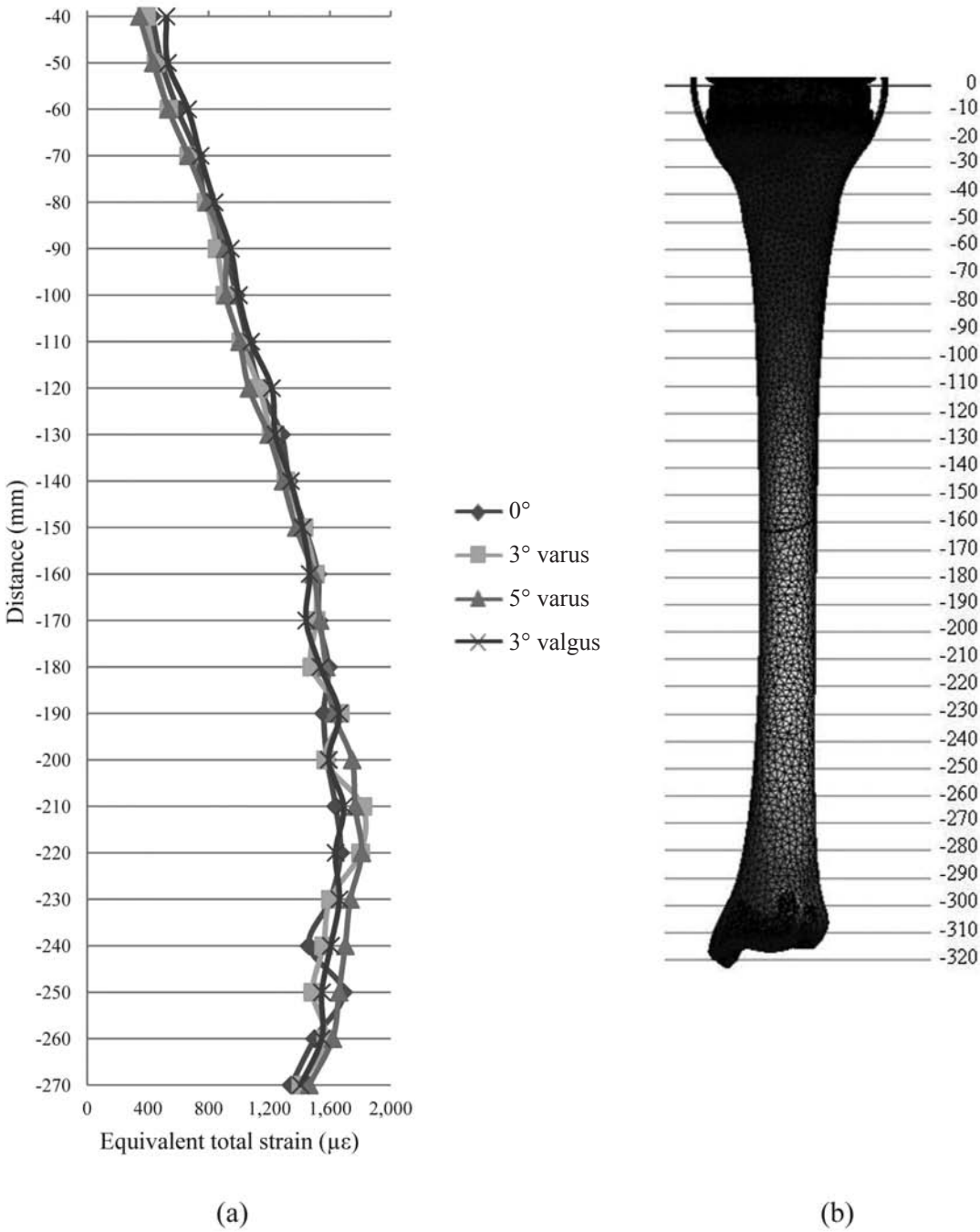

Figure 18 (a) Equivalent total strain on the tibia shaft on posterior side while climbing stairs; (b) Level on tibial bone from proximal to distal part.

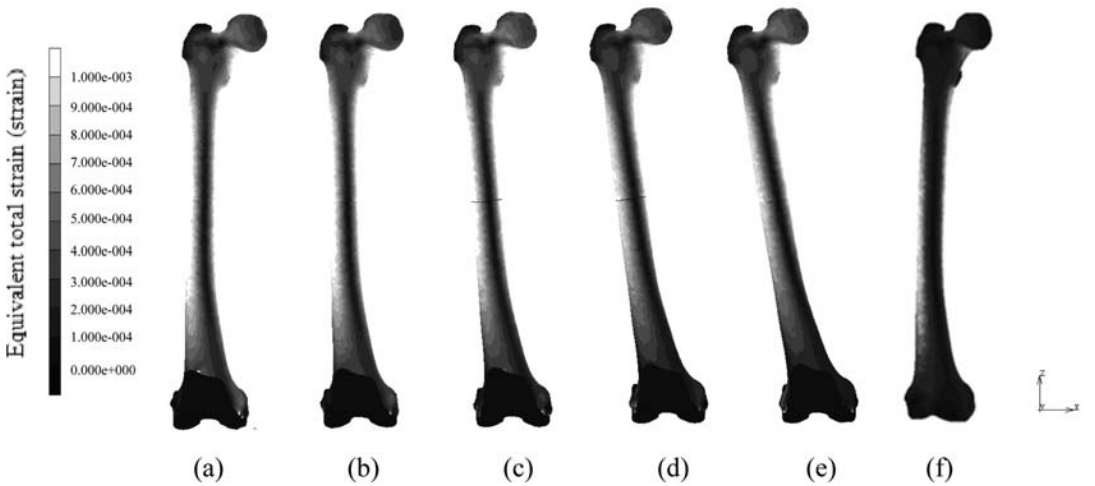

Figure 19 Equivalent total strain on femoral side while walking: (a) Femur with knee prosthesis 5° varus; (b) Femur with knee prosthesis 3° varus; (c) Femur with knee prosthesis 0°; (d) Femur with knee prosthesis 3° valgus; (e) Femur with knee prosthesis 5° valgus; (f) Femur with varus knee.

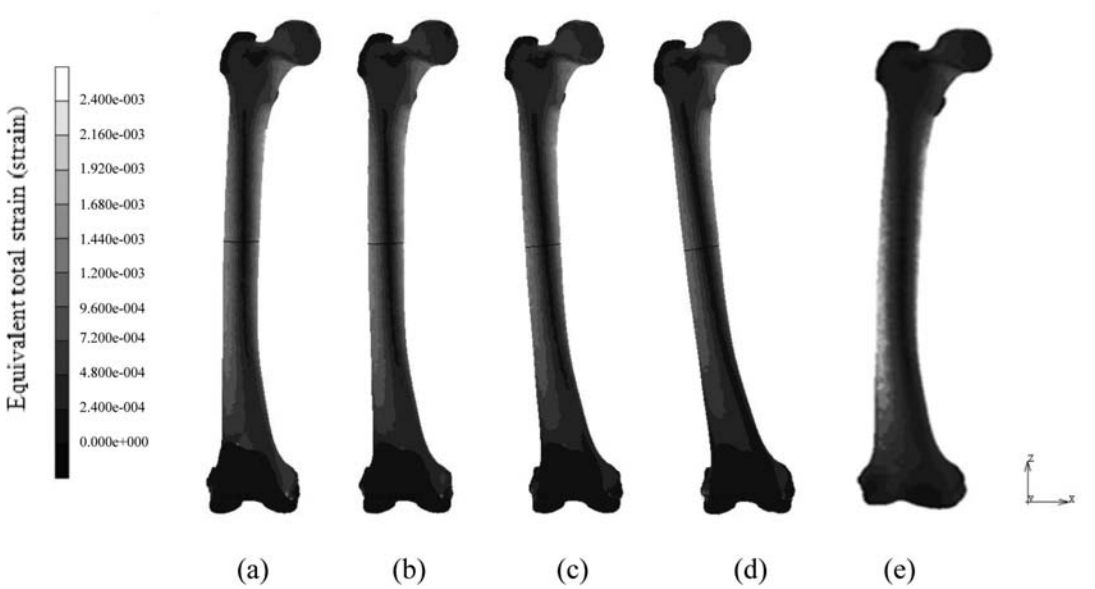

Figure 20 Equivalent total strain on femoral side while climbing stairs: (a) Femur with knee prosthesis 5° varus; (b) Femur with knee prosthesis 3° varus; (c) Femur with knee prosthesis 0°; (d) Femur with knee prosthesis 3° valgus; (e) Femur with varus knee.

Table 4 Average equivalent total strain on the medial side of the femur.

Model	Average equivalent total strain (microstrain)	
	Walking	Climbing stairs
5° varus	1,336	1,547
3° varus	1,284	1,480
0°	1,219	1,403
3°valgus	1,071	1,265
5° valgus	1,044	-
Femur with varus knee	1,690	1,991

Table 5 Average equivalent total strain on the lateral side of the femur.

Model	Average equivalent total strain (microstrain)	
	Walking	Climbing stairs
5° varus	1,043	1,125
3° varus	999	1,112
0°	939	1,037
3°valgus	816	925
5° valgus	765	-
Femur with varus knee	1,421	1,632

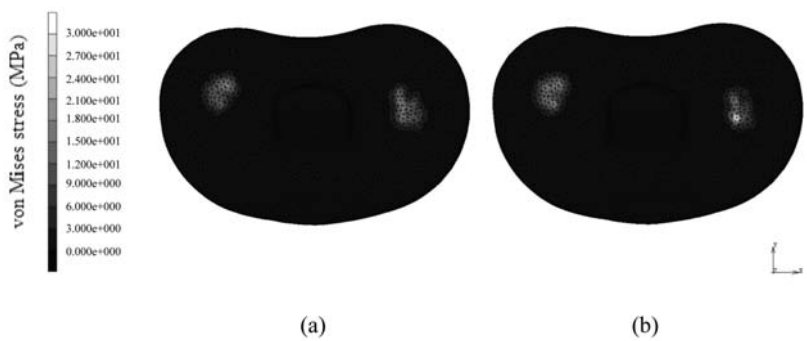

Figure 21 Equivalent von Mises stress on plastic spacer while walking: (a) Model with 0°prosthesis; (b) Model with 3°valgus.

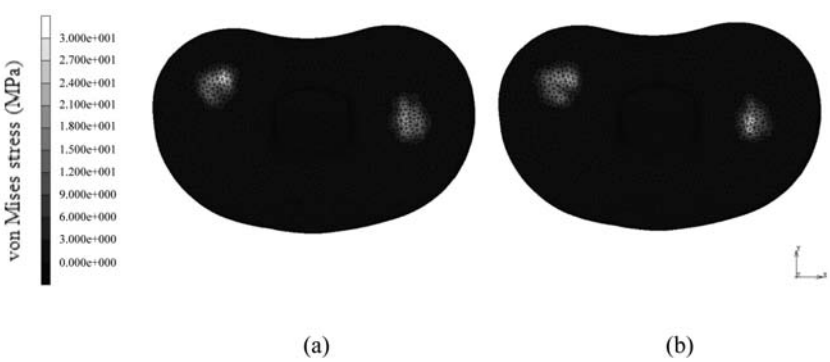

Figure 22 Equivalent von Mises stress on plastic spacer while climbing stairs: (a) Model with 0°prosthesis; (b) Model with 3°valgus.

Tibia bone

The equivalent total strain on the tibia bone using various models is shown in Figures 23 and 24 while walking and climbing stairs, respectively.

The strain distribution on the tibia bone in various models had similar values but occurred in different regions depending on the angle of valgus or varus. In the valgus condition, the strain distributed from the medial side of the bone to the distal part, while in the varus condition, it distributed from the lateral side of the bone to the distal part.

Femoral bone fracture

The results of finite element analysis focused on the strain distribution on the femoral bone under daily activities such as walking and climbing stairs. The graph of Frost's mechanostat theory (Figure 25) shows a strain magnitude greater than 25,000 microstrain on the bone with such values leading to bone fracture (Frost, 1994 and 2003).

The total knee replacement with varus and valgus conditions could help to decrease the strain distribution on the femoral shaft, as it has been shown that the total knee replacement does not affect the risk of a femoral fracture.

CONCLUSION

This research focused on the strain distribution on the thigh bone, especially the strain on the femoral shaft, compared with the effects of different valgus and varus angles of the mechanical axis after insertion of a total knee prosthesis. The total knee arthroplasty did not affect the risk of a femoral fracture. The mechanical axis after total knee arthroplasty had the least equivalent total strain on the bone when the surgeon performs the surgery in 3° valgus but the surgeon should realize this places increased von Mises stress on the medial side of the plastic spacer.

Figure 23 Equivalent total strain on tibia bone while walking: (a) Tibia with knee prosthesis with 5°varus; (b) Tibia with knee prosthesis with 3°varus; (c) Tibia with knee prosthesis 0°; (d) Tibia with knee prosthesis with 3°valgus; (e) Tibia with knee prosthesis 5°valgus.

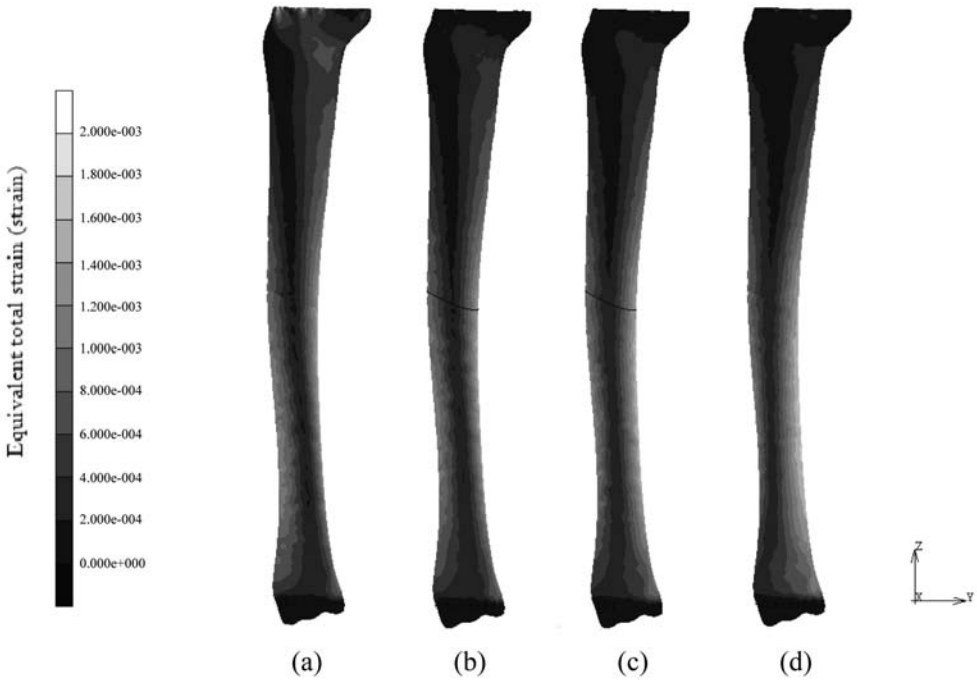

Figure 24 Equivalent total strain on tibia bone while climbing stairs: (a) Tibia with knee prosthesis with 5°varus; (b) Tibia with knee prosthesis with 3°varus; (c) Tibia with knee prosthesis 0°; (d) Tibia with knee prosthesis with 3°valgus.

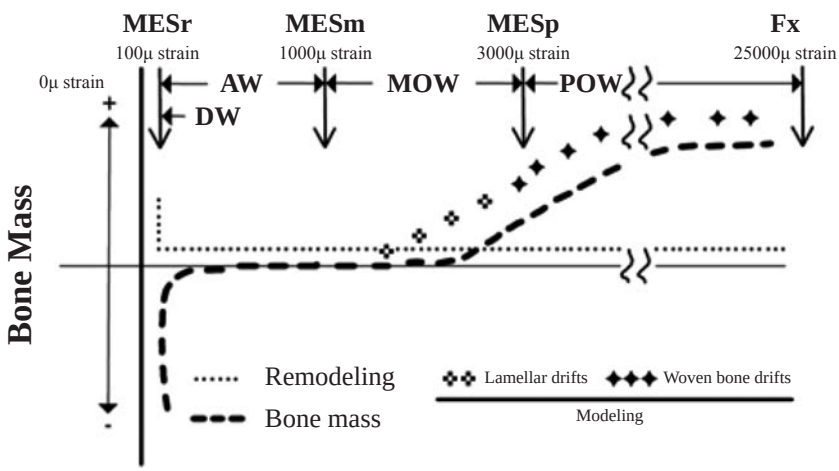

Figure 25 Relationship of strains and adaptive responses (Jee, 2000). MESr = Threshold range for disuse-mode BMU-based bone remodeling; MESm = Bone modeling threshold range (genetic information may encode that threshold in some cell or cells); MESp = Bone operational microdamage threshold range (genetic information may provide that threshold) ("MES" here stands for Minimally Effective Strains or other Stimuli); Fx = Bone fracture strength (ultimate strength); DW = disuse window; AW = adapted window, as in normally adapted young adults; MOW = mild overload window, as in healthy growing mammals; POW = pathologic overload window.

ACKNOWLEDGEMENT

The authors wish to thank the Faculty of Medicine, Burapha University for their support with facilities.

LITERATURE CITED

American Academy of Orthopaedic Surgeons. 2011. **Total Knee Replacement** [Available from: http://orthoinfo.aaos.org/topic.cfm?topic=a00389]. [Sourced 22 January 2013].

Amornsamankul, A., K. Kaorapapong and B. Wiwatanapataphee. 2010. Three-dimensional simulation of femur bone and implant in femoral canal using finite element method. **IJMACS** 4: 171–178.

Basafa, E., R.S. Armiger, M.D. Kutzer, S.M. Belkoff, S.C. Mears and M. Armand. 2013. Patient-specific finite element modeling for femoral bone augmentation. **Med. Eng. & Phy.** 35: 860–865.

Bendjaballah, M.Z., A. Shiraz-Adi and D.J. Zukor. 1997. Finite element analysis of human knee joint in varus-valgus. **Clinical Biomechanics** 12: 139–148.

Daniel, P.A., M.J. Kassim, M. Joe, J. Andrew, N. Michael, C. Cyrus and K.A. Nigel. 2011. Changes in hip fracture rate before and after total knee replacement due to osteoarthritis: A population-based cohort study. **Annals of the Rheumatic Diseases** 70(1): 134–138.

Frost, H.M. 1994. Wolff's law and bone's structural adaptation to mechanical usage: An overview for clinicians. **The Angle Orthodontist** 64(3): 175–188.

Frost, H.M. 2003. A 2003 Update of bone physiology and Wolff's law for clinicians. **Angle Orthodontis** 74: 3–15.

Helgason, B., H. Palsson, T.P. Runarsson, L. Frossard and M. Viceconti. 2009. Risk of failure during gait for direct skeletal attachment of a femoral prosthesis: A finite element study. **Med. Eng. & Phy.** 31: 595–600.

Heller, M.O., G. Bergman, J.P. Kassi, L. Claes, N.P. Hass and G.N. Duda. 2004. Determination of muscle loading at the hip joint for use in pre-clinical testing. **J. Biomechanics** 38(5): 1155–1163.

Jee, W.S. 2000. Principles in bone physiology. **J. Musculoskel Neuron Interact** 1: 11–13.

Mandelbaum, B. and D. Waddell. 2005. Etiology and pathophysiology of osteoarthritis. **Orthopedics** 28(2 Suppl): s207–214.

Nishiyama, K.K., S. Gilchrist, P. Guy, P. Cripton and S.K. Boyd. 2013. Proximal femur bone strength estimated by a computationally fast finite element analysis in a sideways fall configuration. **J. Biomechanics** 46: 1231–1236.

Perez, A., A. Mahar, C. Negus, P. Newton and T. Impelluso. 2008. A computational evaluation of the effect of intramedullary nail material properties on the stabilization of simulated femoral shaft fracture. **J. Med. Eng. & Phys.** 30: 755–760.

Pollard, H., G. Ward, W. Hoskins and K. Hardy. 2008. The effect of a manual therapy knee protocol on osteoarthritic knee pain: A randomised controlled trial. **J. Can Chiropr Assoc.** 52(4): 229–242.

University of Maryland Medical Center. 2011. **Knee Joint Replacement** [Available from http://www.umm.edu/patiented/articles/what_ osteoarthritis_000035_1.html]. [Sourced 22 January 2013].

Weiss, J.A. and J.C. Gardine. 2001. Computational modeling of ligament mechanics. **Critical Review in Biomedical Engineering** 29: 1–70.